Available online at www.sciencedirect.com
ScienceDirect
Ceramics International 34 (2008) 1719–1727
CERAMICS INTERNATIONAL
www.elsevier.com/locate/ceramint

Effects of different production techniques on glass–alumina functionally graded materials

V. Cannillo, L. Lusvarghi, C. Siligardi, A. Sola *

Dipartimento di Ingegneria dei Materiali e dell'Ambiente, University of Modena and Reggio Emilia, Via Vignolese 905, 41100 Modena, Italy

Received 15 November 2006; received in revised form 30 April 2007; accepted 20 May 2007
Available online 19 August 2007

Abstract

Glass–alumina functionally graded materials were obtained using two different methods: percolation, which was representative of natural transport based processes, and plasma spraying, which was representative of constructive processes. The specimens produced in this way were investigated to evaluate the effect of production techniques on the final microstructure and gradient, which, in turn, govern the properties and performances of the graded systems. Moreover, post-production heat treatments were performed in order to improve the reliability of the materials examined.

Keywords: B. Microstructure-final; D. Al_2O_3; D. Glass; Functionally graded materials

1. Introduction

Functionally graded materials (FGMs) are a new class of composite materials, whose composition and microstructure vary in space realising a predetermined law [1–3]. In actual fact, in conventional (not graded) composites, the constituent phases are evenly distributed in space and therefore the properties are – on average – uniform. However, in FGMs, the composition and microstructure vary smoothly in space and the properties and performance therefore also vary from one point to another. The functional gradient can be tailored to the specified service conditions, thus ensuring the best response of the system to the thermo-mechanical load applied, especially if this changes in space. On the other hand, due to the gradual variation of composition and microstructure, it is possible to avoid abrupt interfaces, which may induce local stress concentrations [1]. Moreover, if the gradient is properly designed, FGM performances can be improved compared to conventional composite materials. For example, in glass–alumina FGMs the optimisation of the compositional change may significantly increase the surface resistance to Hertzian cracking compared to conventional (not graded) glass–alumina composites, even if the mean compositions of the graded and not-graded systems are identical [4]. The sliding contact damage can also be substantially reduced [5].

FGMs were first introduced as a clearly defined class of materials in the 1980s and were employed as high performance thermal barrier coatings in spacecraft [6]. Thermal barrier coatings usually couple a highly refractive ceramic phase with a though metallic phase however, if a ceramic layer and a metallic layer are directly coupled, residual stresses are likely to occur at the interface due to the thermo-mechanical mismatch. FGMs were introduced because they made it possible to exploit the thermal stability of the ceramic on one hand and the mechanical properties of the metal on the other, however the distinct interface was replaced by a very gradual change in composition [6]. Due to their vast potential, FGMs are now widely employed in several fields: for example, as protective shields against wear and erosion [7,8]; in electronic devices [9] and biomaterial systems [10].

In order to use FGMs in structural and functional applications, however, a suitable fabrication technique is needed that makes it possible to produce precisely the microstructural and compositional gradient required and assures high reproducibility of the gradient [2]. Production techniques are usually divided in two main groups: ''natural transport based processes'' and ''constructive processes'' [2]. The methods belonging to the former group exploit spontaneous transport phenomena, such as atomic

* Corresponding author. Tel.: +39 059 2056240; fax: +39 059 2056243.
E-mail address: sola.antonella@unimore.it (A. Sola).

0272-8842/$34.00
doi:10.1016/j.ceramint.2007.05.018

species diffusion, liquid infiltration and heat transport. Conversely, in the latter group, the gradient is substantially accumulated through layer-by-layer deposition.

In this work, glass–alumina FGMs were produced using two different methods: percolation, a typical example of a ''natural transport based process'', and plasma spraying, a typical example of a ''constructive process''. Even when the constituent phases were the same, namely alumina and glass, the final microstructures obtained were significantly different. The microstructural peculiarities and the main mechanical properties were subsequently analysed in depth, to investigate the process-microstructure-performance relationship in the resulting glass–alumina FGMs.

2. Experimental

2.1. Constituent phases

The FGMs were made of two ingredient materials: glass and alumina. The glass formulation (CaO: 36.4 wt.%; ZrO_2: 9.1 wt.%; SiO_2: 54.5 wt.%) belonged to the ternary system CaO–ZrO_2–SiO_2 (CZS) [11], which was chosen for several reasons. First, as shown in previous works [11–13], the glasses belonging to this ternary system usually demonstrate good chemical, physical and mechanical properties. ZrO_2 significantly increases the chemical resistance of silicate glasses; both the acid and the alkaline durability may be improved by the addition of even small amounts of ZrO_2 [14]. For the glass used in this study, it has been proven elsewhere that the CaO leaching in bi-distilled stirred water at room temperature is lower than 0.02 mg_{CaO}/g_{glass} [12]. The refractive index is also increased by the ZrO_2: the refractive index of a glass containing CaO 40.0 wt.% and SiO_2 60.0 wt.% (SiO_2/CaO ratio = 1.5) was measured (Becke line method) and found to be 1.600 ± 0.005, however the refractive index of the glass used here (same SiO_2/CaO ratio = 1.5) was 1.630 ± 0.005 [12]. The presence of ZrO_2, which acts as a network former, also influences the glass transition temperature, which is 737 °C for a glass containing CaO 40.0 wt.% and SiO_2 60.0 wt.% [12] and 790 °C for the glass enriched with ZrO_2 [11]. In addition, both the Vickers hardness ($Hv = 671 \pm 59\,kg/mm^2 = 6.58 \pm 0.58$ GPa [11]) and fracture toughness ($K_{IC} = 0.86 \pm 0.13$ MPa $m^{1/2}$ [11]) of the CZS glass considered in this study are relatively high in value for a glass (for an ordinary soda-lime glass, typical values of the Vickers hardness and the fracture toughness – measured from the crack length – are 5.5 GPa [15] and 0.55 MPa $m^{1/2}$, respectively [16]). The Young's modulus of the glass (96 GPa [11]) is also good for a glass (typical values for a soda-lime glass: 70 GPa [17]). Furthermore, with the aim of reducing the thermo-mechanical mismatch between the ingredient materials [18], the coefficient of thermal expansion of the glass could be controlled by a proper design of its formulation (glass: $8.3 \times 10^{-6}\,K^{-1}$; Al_2O_3: $8.7 \times 10^{-6}\,K^{-1}$ [19]). Moreover, the absence of Al_2O_3 in the glass could be useful for characterising the FGM, since the alumina substrate and the glass have completely different compositions.

The glass was investigated thoroughly elsewhere [11], however a brief description of the production process is included here, since it is part of the FGM fabrication. The glass was obtained starting from powdered raw materials, i.e. calcium carbonate (Colorobbia Italia), zirconium silicate (Zircobit FU, Colorobbia Italia), and quartz (Sikron 300, Colorobbia Italia). The powders were weighed, dry mixed and then melted, applying the following heat treatment: from room temperature to 1000 °C at 10 °C/min; 1 h at 1000 °C, to allow the decomposition of the calcium carbonate; from 1000 °C to 1550 °C at 10 °C/min; 1 h at 1550 °C, to homogenise the temperature of the batch. After that, some glass was poured into a mould, in order to obtain a bulk specimen, which was annealed at 800 °C for 1 h and then slowly cooled inside the kiln. The remaining glass was plunged into cold water (room temperature), in order to obtain a frit, which was wet ball-milled and dried in a kiln. The glass bulk was cut into small, flat pieces (about 8 mm × 8 mm × 1 mm) and used to fabricate the percolated FGM. The glass powder, on the other hand, was spray dried (NIRO Atomizer, Denmark, located at Centro Sviluppo Materiali – CSM – Roma, Italy) and used to produce the plasma sprayed FGMs.

Both the percolated and the plasma sprayed FGMs were obtained using alumina tiles as substrate [20]. The alumina, a commercially available product (Keramo Ceramiche Tecniche, Tavernerio (CO), Italy), showed a fine-grained polycrystalline microstructure, with a small residual porosity (about 5.5 vol.%). A commercial alumina powder (Sulzer Metco 105SFP) was also used to produce the plasma sprayed FGMs. Both the alumina substrates and the alumina powder were analysed by X-ray diffraction (XRD—X'Pert Pro PANalytical), which confirmed the presence of only one crystal phase, i.e. a rhombohedral structured Al_2O_3 (α-alumina) [20].

2.2. Functionally graded materials

As already mentioned, the samples were prepared using two different methods: percolation and plasma spraying.

In order to obtain the percolated FGM, labelled as ''FGM-perc'', a piece of glass was placed on the top surface of an alumina body, then a suitable heat treatment was performed that caused the glass to melt and infiltrate the polycrystalline alumina. The heating cycle is graphically represented in Fig. 1.

To produce the plasma sprayed FGMs [20], on the other hand, the alumina substrates were previously grit blasted with SiC powder (mean grain size: 165 μm; Zamboni Luciano, Montichiari (BS) Italy—Provider) by using a vacuum-operated Norblast blasting machine equipped with a hand-held blasting gun (internal diameter 8 mm) and slightly pre-heated to about 150 °C. The graded coatings were then deposited on the thus-prepared alumina substrates by spraying several layers of progressively different composition: in the sample labelled as ''FGM-PS1'' the mean composition varied from 100 vol.% alumina at the interface with the substrate to 100 vol.% glass at the outer top surface; in ''FGM-PS2'' the mean composition varied from 80 vol.% alumina–20 vol.% glass at the interface to 100 vol.% glass at the surface, as shown in Fig. 2. It is worth

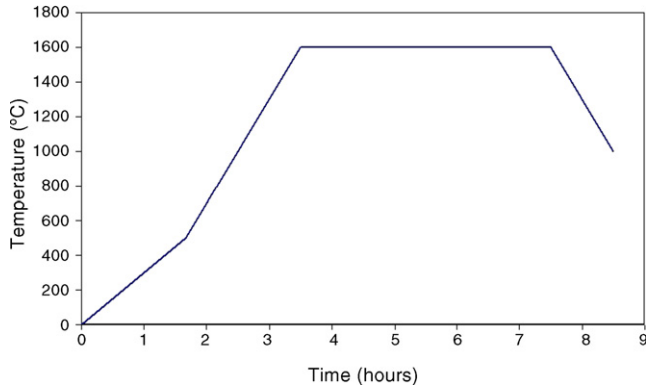

Fig. 1. Heat treatment required to induce the glass penetration into the alumina substrate.

noting that the glass powder and the alumina were not premixed in fixed proportions, but rather they were separately and simultaneously introduced in the plasma flux by two different feeders [20]. The compositional gradient, in fact, was created by gradually changing the feeding flow rate of the two powders. The feeding flow rate of the powders was calculated for each layer on the basis of a preliminary deposition efficiency measurement: basically, a fixed amount of each type of powder (glass; alumina) was deposited singly on an alumina substrate under the same spraying conditions and number of torch passes and the thickness of the two coatings was then measured and used to calibrate the respective flow rate during FGM fabrication [20].

All the spray runs were performed using a F4-MB plasma torch installed in a Controlled Atmosphere Plasma-Spraying plant (co-shared with Università "La Sapienza", Roma, Italy) at Centro Sviluppo Materiali S.p.A. (Roma, Italy), however, both the graded coatings were sprayed in APS mode. In order to obtain the system FGM-PS1, 21 layers were deposited; in order to obtain the system FGM-PS2, 17 layers were required (as shown in Fig. 2). In both cases, the layer thickness was kept constant (about 30 μm).

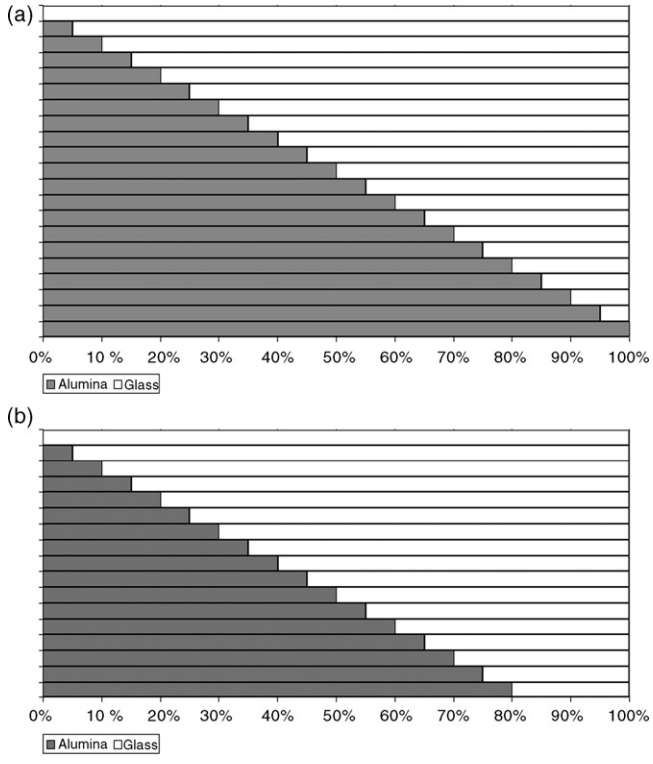

Fig. 2. Diagram of the composition of the graded coatings deposited on the alumina substrate in FGM-PS1 (a) and in FGM-PS2 (b).

In order to investigate the different microstructures resulting from percolation and plasma spraying, the surface (unpolished) and the cross-section (polished) of the three systems, FGM-perc, FGM-PS1, and FGM-PS2, were observed with a Scanning Electron Microscope (SEM—Philips XL-30). X-ray energy dispersion spectroscopy (X-EDS) analysis, aimed at defining the maximum depth reached by the glass, was also performed on the FGM-perc cross-section.

Since the high temperatures of the fabrication methods could induce crystallization phenomena and/or polymorphous transformations, a mineralogical study was carried out on the surface and the cross-section of the FGM samples. In particular, in order to minimise the signal from the alumina substrate during the cross-section investigation, the X-ray (XRD—X'Pert Pro PANalytical) beam was focused on the graded area using a 300 μm slid.

Besides the microstructural and mineralogical characterisation of the percolated and the plasma sprayed FGMs, a Vickers micro-indentation test (Vickers Indenter, Open Platform, CSM Instruments) was performed on the cross-section of the three specimens in order to evaluate the hardness as a function of depth. The maximum applied load was set to 10 N for the percolated FGM and to 1 N for the plasma sprayed FGMs. The results were therefore unsuitable for a direct quantitative comparison, but were useful for appreciating the functional gradient associated to the compositional and microstructural change. The indenter automatically determined the instrumental hardness, H_{it}, which was defined as the ratio between the maximum applied load, F_{max}, and the projected contact area, h_c:

$$H_{it} = \frac{F_{max}}{h_c} \quad [\text{Pa}]$$

In order to evaluate the resistance of the FGMs, a qualitative fracture test was performed: bar shaped specimens (about 50 mm × 8 mm × 5 mm) were notched (to about 2 mm of depth) on the opposite side with respect to the graded surface and bent to break, the fracture surfaces were then observed with the SEM.

3. Results and discussion

At the end of the heat treatment, the FGM-perc sample showed some residual glass on its top surface. This layer of pure glass was extremely smooth, because during the thermal treatment the glass melted and then remained amorphous. The top surface of FGM-PS1 and FGM-PS2, however, was extremely rough, due to its particular microstructure. At the SEM observation, the top surface of both FGM-PS1 and FGM-PS2 revealed a splat-like morphology that is common in plasma

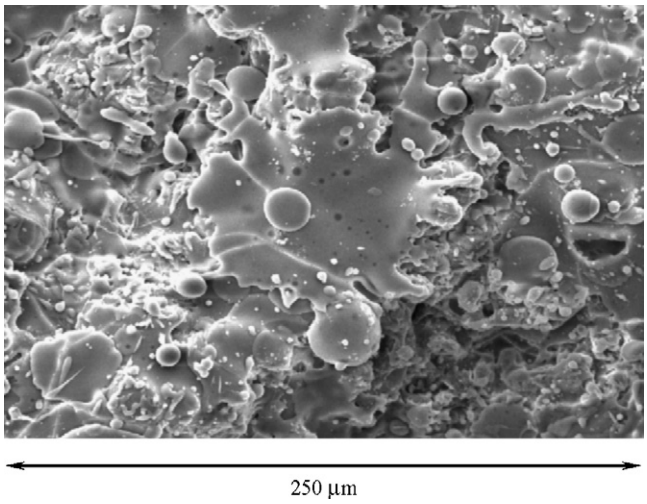

Fig. 3. Surface microstructure of FGM-PS1.

sprayed systems [21], as shown in Fig. 3. This image suggests that some droplets of molten glass splashed and broke up while impacting on the previously deposited layers, creating secondary spherical droplets. Therefore, although the top surface was made of glass in all the samples, the microstructure was quite different in the percolated system and the plasma sprayed ones.

The microstructural differences were confirmed by the SEM investigation of the cross-sections. As regards the FGM-perc sample, although some residual glass remained on the top surface, the glass progressively infiltrated the alumina polycrystalline body by moving along its grain boundaries and partially filling its pores [11], as shown in Fig. 4(a). In this picture, the white areas are glass and the dark grey areas are alumina (as demonstrated by the X-EDS analysis). The FGM-perc microstructure smoothly changes along the glass percolation direction until, at a depth of about 1600–1700 μm, the white areas formed by the glass are no longer visible, as shown in Fig. 4(b). On the other hand, X-EDS analysis was able to detect some Si (considered as a marker of the glass) down to a depth of about 1600 μm, which was assumed as the maximum depth reached by the glass. Two points are worth noting. First of all, in the FGM-perc cross-section it was not possible to detect a clearly defined interface between the area interested by the glass percolation and the underlying pure alumina; in other words, the glass infiltration resulted in a very gradual compositional change, since the glass content progressively decreased from the glass-rich superficial area (SiO_2: 35 mol% by X-EDS measurement [22]) to the pure alumina area at a depth of about 1600 μm, where the glass did not reach (SiO_2: 0 mol% by X-EDS measurement [22]); the linear trend of the compositional profile was confirmed by image processing [19]. However, although the compositional and microstructural gradient was continuous when considered at the dimensional level of the gradient (dimensional scale: hundreds of microns), the microstructure was intrinsically heterogeneous and discrete at the microscale (dimensional scale: tens of microns), since it was possible to distinguish the glass domains and the alumina ones [11,18].

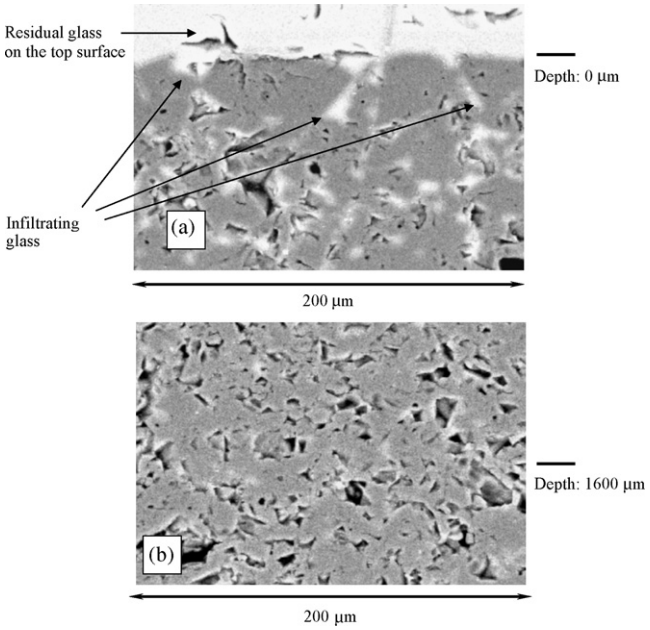

Fig. 4. FGM-perc cross-section at about 0 μm (a) and 1600 μm (b) of depth along the glass percolation direction (white: glass; grey: alumina).

As far as the plasma sprayed systems are concerned [20], the inspection of the cross-section immediately revealed that the graded coating was thicker in FGM-PS1 than in FGM-PS2 (about 700 μm and 500 μm respectively), as shown in Fig. 5(a) and (b). This is reasonable, since the layer thickness was constant and was the same in both samples, however the number of layers was different: 21 in FGM-PS1 and 17 in FGM-PS2.

In both FGM-PS1 and in FGM-PS2, the microstructure appeared mainly lamellar, as is usual in plasma sprayed systems [21]. However, some glass particles maintained a rounded shape which is typical of partially molten glass droplets; the presence of these scarcely flattened particles may be due to the low thermal conductivity of the glass, combined with its relatively high viscosity – if compared to a previously crystalline molten phase – and its relatively low velocity in the plasma flux, caused by its low density [20]. Although the glass and alumina particles were clearly distinguished (white: glass; grey: alumina, see Fig. 5), their interface was relatively good, as shown in Fig. 6.

It is worth noting that the plasma sprayed FGMs were fabricated as multi-layered systems, by depositing several strata whose mean composition was progressively changed; nevertheless the fixed layer thickness was extremely small (about 28–30 μm) and it was therefore comparable with the characteristic microstructural unit size of the system, represented by the splat dimension. Consequently, in both FGM-PS1 and FGM-PS2, it was impossible to identify the single layers [3,23]. In other words, in the plasma sprayed FGMs the overall final gradient was continuous and not step-wise. However, as already mentioned for the percolated FGM, the microstructure was discrete and stochastic, with distinct domains of glass and alumina [20].

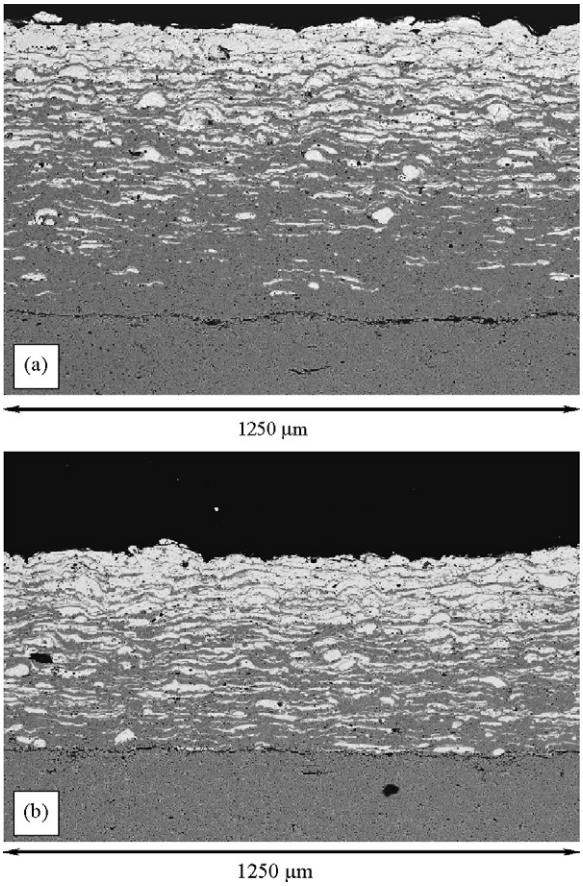

Fig. 5. Cross-section of samples FGM-PS1 (a) and FGM-PS2 (b).

If compared to the percolated FGM, the plasma sprayed systems looked more defective, due to their residual porosity and micro-cracks. In order to evaluate the residual porosity as a function of depth in the three systems in question, for each material several SEM images of the polished cross-section were acquired, arranged to form a mosaic and processed. As shown in Fig. 7, the porosity volume fraction was very low in the percolated FGM (<2 vol.%), but it was much higher in FGM-PS1 and in FGM-PS2 (>4 vol.%). In particular, the residual

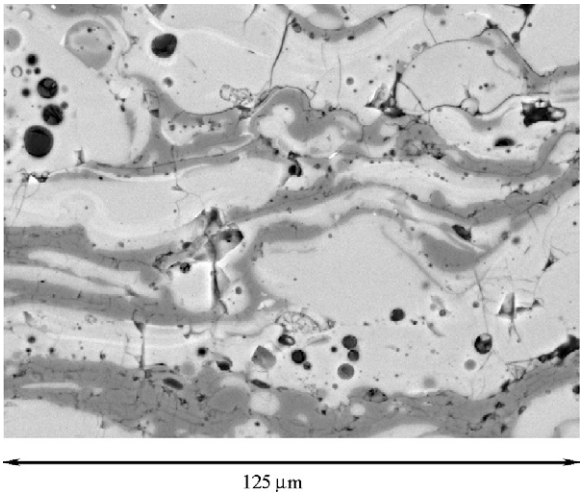

Fig. 6. Interface between glass and alumina splats in plasma sprayed FGMs.

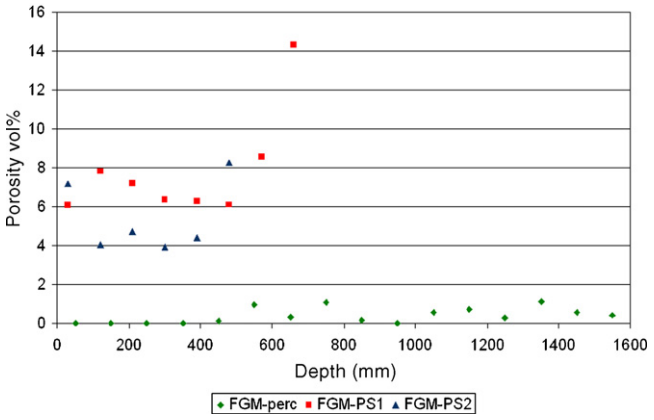

Fig. 7. Porosity as a function of depth in FGM-perc, FGM-PS1 and FGM-PS2.

porosity in the plasma sprayed FGMs (both PS1and PS2) significantly increased at the coating-substrate interface, due to interface defectiveness. The weakness of the interface, which is highlighted in Fig. 5, was a major problem in FGM-PS1 and FGM-PS2.

On the other hand, the intrinsic weakness of the plasma sprayed materials compared to the percolated FGM was confirmed by the hardness measurement shown below. Moreover, previous studies dedicated to the elastic properties of glass–alumina FGMs [19] had proven that the elastic properties of the percolated FGM were higher than those of the plasma sprayed materials (from 290 to 380 GPa in the percolated FGM; from 90 to 220 GPa in a system analogous to FGM-PS1 and from 90 to 200 GPa in a system analogous to FGM-PS2 [19]).

The mineralogical analysis of the FGM-perc top surface confirmed the presence of a layer of residual glass and no crystal phase was visible (not even the underlying alumina substrate). The same result was obtained from FGM-PS1 and FGM-PS2, which were fabricated by depositing pure glass on their top surface. As regards the cross-section, the FGM-perc pattern, which is shown in Fig. 8, was dominated by the α-alumina peaks and no other relevant signals could be detected. This suggests that the glass percolation and the heat treatment did not induce significant crystallisation phenomena or polymorphous transformations. Instead, the spectra of the plasma sprayed specimens, which were quite similar as shown

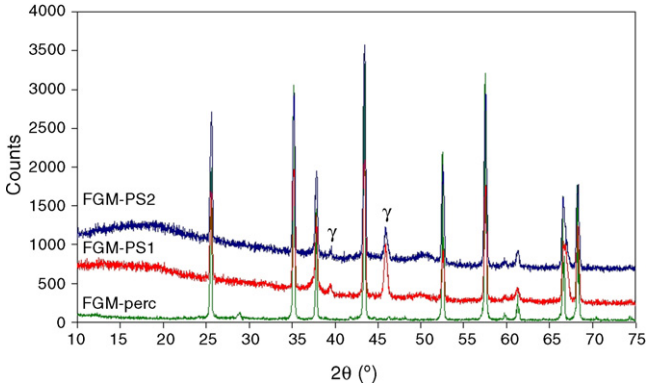

Fig. 8. XRD patterns of the three FGM cross-sections.

in Fig. 8, revealed the presence of two different alumina polymorphs: a cubic one (γ-alumina) and a rhombohedral one (α-alumina). The former was caused by the polymorphous transformation of the α-alumina powder used in the plasma spray process [24]; the latter was due to some sprayed α-alumina particles not transformed into the γ form and to the alumina substrate, whose signal was not completely cut off. However, the mineralogical analysis did not make it possible to detect new crystal phases generated by a glass devetrification or a glass–alumina interaction. The XRD spectra of the plasma sprayed samples suggested that the amorphous phase was more abundant compared to FGM-perc. This may be due to two main reasons: first of all, it is likely that the gradient in the plasma sprayed systems actually contains more glassy phase than the percolated sample; secondly, some sprayed alumina may be in an amorphous state [24,25].

In the microindentation tests, as mentioned previously, two different loads were applied, 10 N for the percolated FGM and 1 N for the plasma sprayed FGMs, the difference being due to the different microstructural strength of the two classes of materials. The results obtained from the samples FGM-PS1 and FGM-PS2 could therefore be directly compared, however this comparison could not be extended to the percolated FGM. Nevertheless, the main target of this test was to highlight the functional gradient that arose as a consequence of the microstructural and compositional gradient. As shown in Fig. 9, in the cross-section of FGM-perc (Fig. 9(a)) the instrumental hardness (H_{it}) became progressively greater as a function of depth due to the increasing alumina content, until it reached the value typical of the pure alumina at a depth of about 1600 μm. This was consistent with the SEM and X-EDS findings, which revealed a smooth variation in composition with a maximum depth reached by the glass of about 1600 μm. Again, in the plasma sprayed samples (Fig. 9(b)) the instrumental hardness increased as a function of depth and, down to a depth of about 460 μm, its value was almost the same – at the same depth – in the two specimens. In fact, as mentioned above, if the first 500 μm of depth are considered, the compositional change rate was the same in FGM-PS1 and FGM-PS2 and therefore the alumina content and the glass one were the same at the same depth, as shown in Fig. 2. However, the instrumental hardness at about 460 μm was significantly lower in FGM-PS2 than in FGM-PS1: this was probably due to the influence of the interface that, as mentioned above, was somewhat defective. On the other hand, the instrumental hardness of FGM-PS1 also apparently decreased from a depth of 540–620 μm, despite the fact that the alumina content was increasing, possibly as a consequence of the weakening effect of the interface in this case, too. The properties and performances, such as instrumental hardness, were not actually governed by the local composition of the graded system alone, but also by the microstructural features, such as defects and pores.

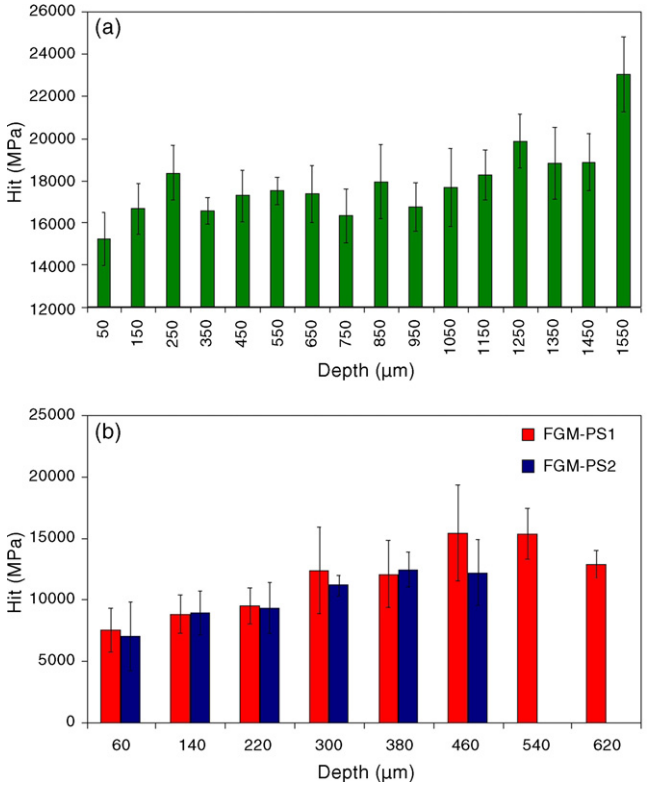

Fig. 9. Instrumental hardness as a function of depth in FGM-perc (a) and in FGM-PS1 and FGM-PS2 (b).

The fracture tests confirmed the relevance of such microstructural peculiarities and, in particular, of interface adhesion. In FGM-perc, where the glass infiltration resulted in a very gradual compositional gradient and there was no distinct interface between the graded area of the cross-section and the underlying pure alumina not infiltrated by the glass, the fracture test did not cause any delamination and the fracture surface suggested that cracks preferentially originated from residual pores (not filled by the glass) and propagated through glass domains [26,27]. Fig. 10(a) shows a detail of the fracture surface in FGM-perc, where the smooth areas indicated by the arrows were generated by crack propagation through glass domains. In FGM-PS1, where the interface was particularly defective, the graded coating spalled out before breaking [27], as proved by Fig. 10(b). Conversely, in FGM-PS2, interface adhesion was improved by the presence of some glass (at least 20 vol.%), which probably acted as a bonding agent during the coating build-up; consequently, the coating did not immediately break off and system failure was due to the concurrent phenomena of interface delamination and crack propagation from pores and other microstructural defects [27], as shown by the detail in Fig. 10(c).

4. Further developments

The percolation method proved to be relatively easy and suitable for obtaining reliable materials, since the progressive infiltration of the glass into the alumina substrate created a smooth compositional and microstructural gradient, without any clearly defined interface. Nevertheless, percolation, which is a natural transport based process, does not guarantee either high reproducibility or great flexibility. According to Kuromitsu et al. [28], if it is assumed that the driving force for infiltration is capillarity, it is possible to predict the maximum

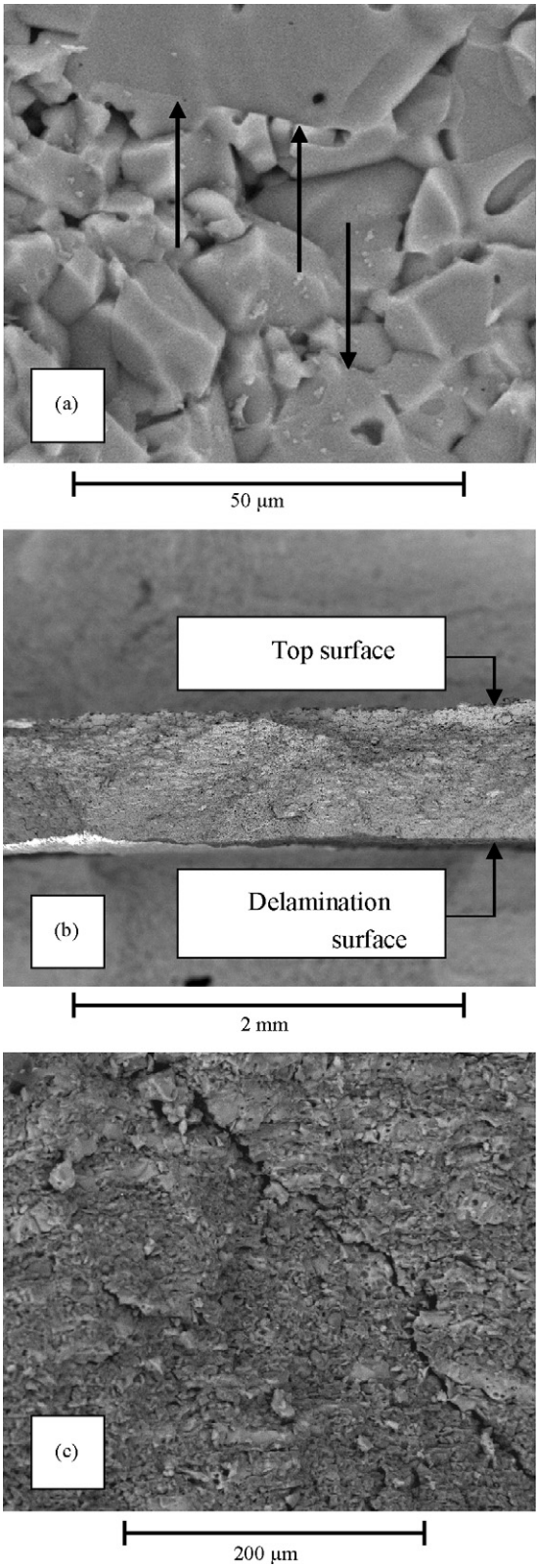

Fig. 10. Fracture tests in FGM-perc (a), FGM-PS1 (b) and FGM-PS2 (c).

depth reached by the glass as a function of the fabrication parameters, such as time and temperature, but it is not possible to arbitrarily build the gradient.

On the contrary, the plasma spraying method, which is a constructive technique, can be used to plan and faithfully achieve a vast assortment of gradients. However, in this work, the thus-produced FGMs were penalised by poor adhesion between the graded coating and the alumina substrate. In order to improve the reliability of the plasma sprayed FGMs, the creation of a proper compositional gradient proved to be useful. In actual fact, the direct observation and testing of the two plasma sprayed systems considered here suggested that the presence of some glass at the interface could be favourable, since the glass droplets in the molten state could act as a bonding agent during the deposition process.

A further improvement was achieved by means of a suitable thermal treatment [20]. On the basis of previous investigations on the sintering and crystallization of plasma sprayed CZS glass systems [20,29], a sample of each type (FGM-PS1 and FGM-PS2) was heat treated at 850 °C for 30 min and then at 1050 °C for a further 30 min. At the end of the thermal treatment, the coating spalled out from the FGM-PS1 sample, but remained stuck in the FGM-PS2 one. Moreover, in FGM-PS2 the interface looked far better after the thermal treatment, as shown in Fig. 11. The different behaviour of the sprayed systems was due to the coating-substrate adhesion, which was stronger in FGM-PS2 than in FGM-PS1 (especially at high temperature) thanks to the presence of some glass at the interface, and to the coating thickness, which was smaller in FGM-PS2 than in FGM-PS1, thus resulting in lower residual stresses. The heat-treated FGM-PS2 sample was further studied. The SEM investigation demonstrated that the glass sintered and crystallized during the heat treatment, as shown in Fig. 12. Therefore, in order to identify the new crystal phases, XRD analysis was performed on both the cross-section and the surface of the sample: in this way, it was possible to identify – both on the top surface and the cross-section – a wollastonite phase, wollastonite-2M (JCPDS-ICDD 00-027-0088), which is extremely common in the crystallization processes of CZS glasses [11,12]. Fig. 13 shows a comparison between the XRD patterns collected on the FGM-PS2 top surface before and after the heat treatment. The top surface of the sample was also subject to a scratch test (Open Platform, CSM Instruments)

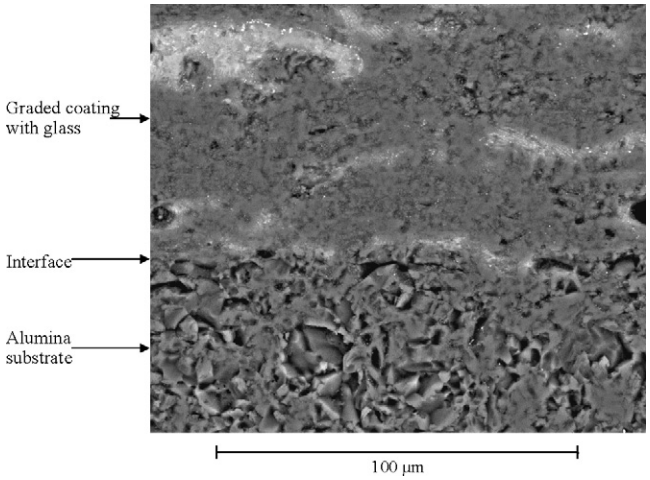

Fig. 11. Interface between the graded coating and the alumina substrate in FGM-PS2 after the thermal treatment.

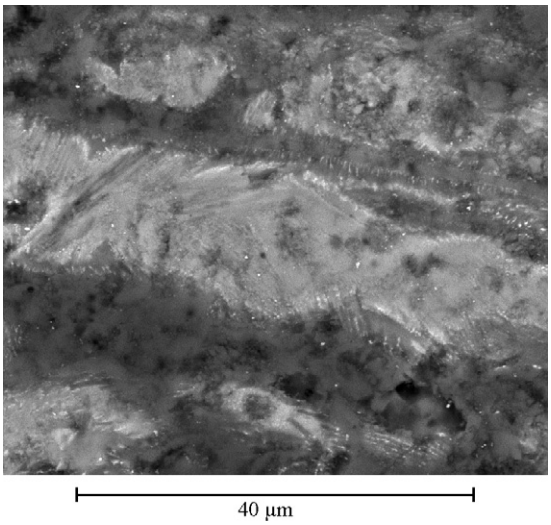

Fig. 12. Sintered and crystallized glass in FGM-PS2 (cross-section) after the thermal treatment.

using a Rockwell diamond indenter (radius 200 μm) before and after the thermal treatment. The load was progressively increased from 1 to 30 N with a loading rate of 14.5 N/min and the scratch length was set to 1 mm. In order to establish a benchmark, the same test was also repeated on the percolated FGM (some superficial glass was removed in order to test the graded material). This test made it possible to appreciate the surface resistance to damage. From the images in Fig. 14, it is possible to deduce that the progressive scratch severely damaged the as sprayed FGM-PS2 sample (Fig. 14(a)), however, superficial resistance was significantly increased by the heat treatment, which is demonstrated by the fact that the damage in the heat treated sample (Fig. 14(b)) was very small and comparable with that in the percolated system (Fig. 14(c)), even at high loads. In order to quantify the results of the scratch tests, the scratches are usually measured by means of a profilometer; in this case, however, this technique was not feasible, due to the superficial roughness of the specimens, which was particularly evident in the as-sprayed FGM-PS2 sample. On the other hand, it was not possible to perform preliminary polishing, because this would have removed the superficial layers of the graded coating, thus altering the systems examined. Therefore, a quantitative evaluation was

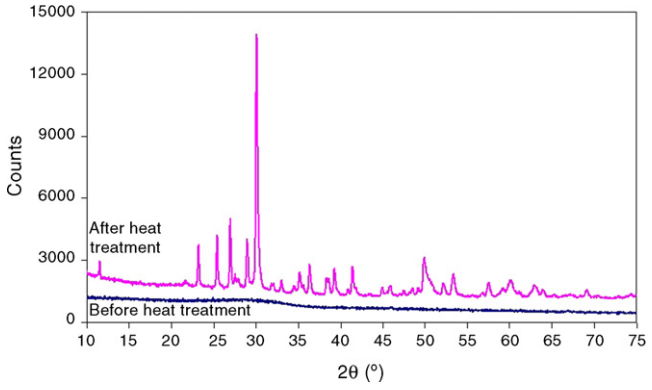

Fig. 13. XRD patterns of the FGM-PS2 top surface before and after the heat treatment.

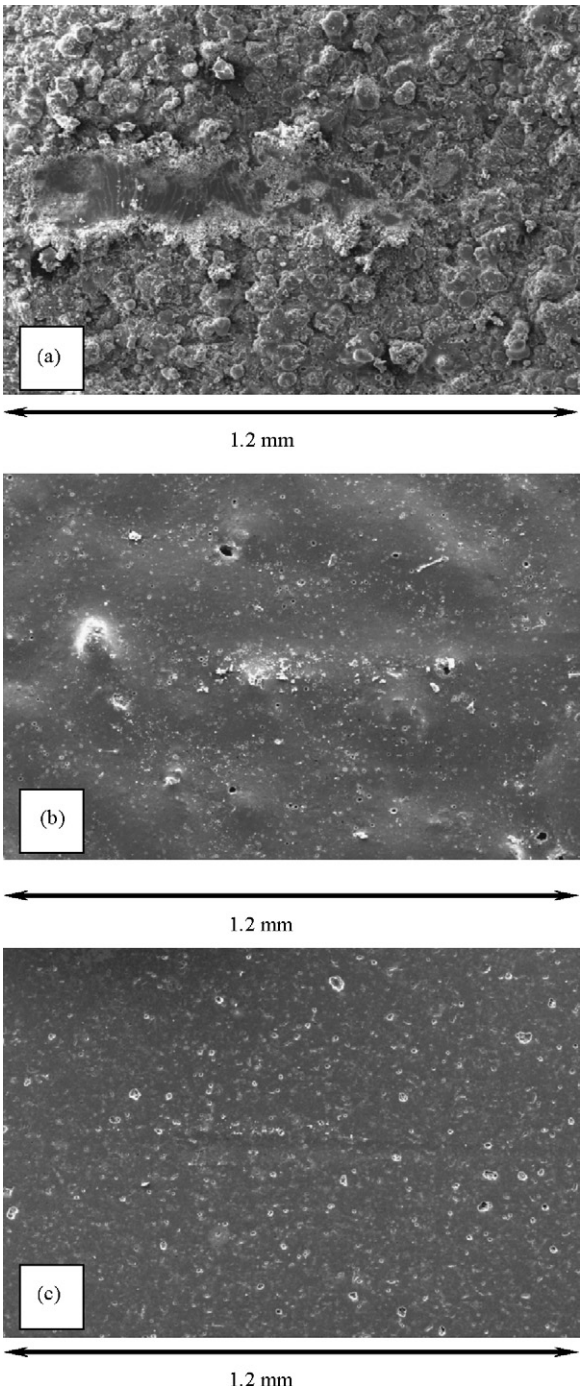

Fig. 14. Scratch tests on the top surface of FGM-PS2 before the heat treatment (a), FGM-PS2 after the heat treatment (b), and FGM-perc (c).

obtained by measuring the width of the progressive scratches on the three samples; the data, which are comparable due to the brittle behaviour of all the materials considered, were collected on the point of the scratch corresponding to the maximum applied load (30 N). The width of the scratch proved to be about 150 μm in the as-sprayed FGM-PS2 sample, 65 μm in the heat-treated FGM-PS2 sample and 70 μm in the percolated FGM. As shown in Fig. 14, however, the measurement of the scratch of the heat-treated plasma-sprayed FGM was difficult, because the scratch could be seen hardly, although the applied load was

30 N (instrumental limit). The heat treatment, therefore, made it possible to strengthen the plasma sprayed system.

5. Conclusions

Both percolation and plasma spraying could be successfully employed to produce glass alumina FGMs. In particular, the former is a typical example of a natural transport based process, which proved to be relatively easy and made it possible to obtain very smooth compositional gradients. However, this method lacked flexibility, since the compositional and microstructural gradient could not be arbitrarily designed. The latter technique, plasma spraying, is a classical example of a constructive technique, since the gradient was literally built up layer by layer. Plasma spraying made it possible to obtain a wide variety of gradients, which could be accurately achieved. Nevertheless, the plasma sprayed FGMs considered here were characterised by a defective coating-substrate interface. The adhesion could be improved by a proper gradient design, with some glass adjacent to the interface, because the glass (in the molten state) acted as a bonding agent during the deposition process. Moreover, if some glass was present at the interface, the reliability of the graded system could be further improved by means of a thermal treatment. The heat treatment, in fact, bettered the interface and induced a controlled sintering and crystallization of the glassy phase: the final system, a new ceramic/glass–ceramic graded material, showed a superficial strength comparable to that of the percolated FGM.

Acknowledgements

This work was co-financed by PRRIITT (Regione Emilia-Romagna), Net-Lab "Surface & Coatings for Advanced Mechanics and Nanomechanics" (SUP&RMAN).

Centro Sviluppo Materiali (CSM) S.p.A. (Roma, Italy), Surface Engineering Unit, kindly performed the spraying sessions. We are also grateful to Mr. Giovanni Bolelli (Dipartimento di Ingegneria dei Materiali e dell'Ambiente, Università di Modena e Reggio Emilia, Italy) for his precious help in the coatings design.

References

[1] A. Kawasaki, R. Watanabe, Concept and P/M fabrication of functionally graded materials, Ceram. Int. 23 (1997) 73–83.
[2] A. Mortensen, S. Suresh, Functionally graded metals and metal-ceramic composites. I. Processing, Int. Mater. Rev. 40 (6) (1995) 239–265.
[3] Y. Miyamoto, W.A. Kaysser, B.H. Rabin, A. Kawasaki, R.G. Ford, Functionally Graded Materials. Design, Processing and Applications, Kluwer Academic Publishers, 1999.
[4] J. Jitcharoen, N.P. Padture, A.E. Giannakopoulos, S. Suresh, Hertzian-crack suppression in ceramics with elastic-modulus-graded surfaces, J. Am. Ceram. Soc. 81 (9) (1998) 2301–2308.
[5] S. Suresh, M. Olsson, A.E. Giannakopoulos, N.P. Padture, J. Jitcharoen, Engineering the resistance to sliding-contact damage through controlled gradients in elastic properties at contact surfaces, Acta Mater. 47 (14) (1999) 3915–3926.
[6] M. Koizumi, M. Niino, Overview of FGM research in Japan, MRS Bull. 1 (1995) 19–21.
[7] L. Prchlik, S. Sampath, J. Gutleber, G. Bancke, A.W. Ruff, Friction and wear properties of WC–Co and Mo–Mo_2C based functionally graded materials, Wear 249 (12) (2001) 1103–1115.
[8] H.X. Zhao, M. Yamamoto, M. Matsumura, Slurry erosion properties of ceramic coatings and functionally gradient materials, Wear 186–187 (2) (1995) 473–479.
[9] E. Müller, Č. Drašar, J. Schilz, W.A. Kaysser, Functionally graded materials for sensor and energy applications, Mater. Sci. Eng. A 362 (1–2) (2003) 17–39.
[10] R. Roop Kumar, M. Wang, Functionally graded bioactive coatings of hydroxyapatite-titanium oxide composite system, Mater. Lett. 55 (2002) 133–137.
[11] V. Cannillo, T. Manfredini, M. Montorsi, C. Siligardi, A. Sola, Glass–alumina functionally graded materials: their preparation and compositional profile evaluation, J. Eur. Ceram. Soc. 26 (13) (2006) 2685–2693.
[12] C. Leonelli, C. Siligardi, CaO–SiO_2–ZrO_2 glasses: modelling and experimental approach, Rec. Res. Dev. Mater. Sci. 3 (2002) 599–618.
[13] V. Cannillo, T. Manfredini, C. Siligardi, A. Sola, Preparation and experimental characterization of glass–alumina functionally graded materials, J. Eur. Ceram. Soc. 26 (6) (2006) 993–1001.
[14] A.K. Varshneya, Fundamentals of Inorganic Glasses, Academic Press Inc., New York, 1994.
[15] J. Gong, Y. Chen, C. Li, Statistical analysis of fracture toughness of soda-lime glass determined by indentation (short communication), J. Non-Cryst. Solids 279 (2001) 219–223.
[16] Z. Burghard, A. Zimmermann, J. Rödel, F. Aldinger, B.R. Lawn, Crack opening profiles of indentation cracks in normal and anomalous glasses, Acta Mater. 52 (2004) 293–297.
[17] J.M.F. Navarro, El Vidrio, C.S.I.C., Madrid, 1991.
[18] V. Cannillo, G. de Portu, L. Micele, M. Montorsi, G. Pezzotti, C. Siligardi, A. Sola, Microscale computational simulation and experimental measurement of thermal residual stresses in glass–alumina functionally graded materials, J. Eur. Ceram. Soc. 26 (8) (2006) 1411–1419.
[19] V. Cannillo, L. Lusvarghi, C. Siligardi, A. Sola, Prediction of the elastic properties profile in glass–alumina functionally graded materials, J. Eur. Ceram. Soc. 27 (2007) 2393–2400.
[20] V. Cannillo, L. Lusvarghi, M. Montorsi, C. Siligardi, A. Sola, Characterization of glass–alumina functionally graded coatings obtained by plasma spraying, J. Eur. Ceram. Soc. 27 (2007) 1935–1943.
[21] J.R. Davis (Ed.), Handbook of Thermal Spray Technology, Davis & Associates, ASM International, 2004.
[22] V. Cannillo, L. Lusvarghi, T. Manfredini, M. Montorsi, C. Siligardi, A. Sola, Glass–ceramic functionally graded materials produced with different methods, J. Eur. Ceram. Soc. 27 (2007) 1293–1298.
[23] A. Mortensen, S. Suresh, Functionally graded metals and metal–ceramic composites. II. Thermomechanical behaviour, Int. Mater. Rev. 42 (3) (1997) 85–116.
[24] R.J. Damani, A. Wanner, Microstructure and elastic properties of plasma-sprayed alumina, J. Mater. Sci. 35 (2000) 4307–4318.
[25] G. Bolelli, V. Cannillo, L. Lusvarghi, T. Manfredini, Wear behaviour of thermally sprayed ceramic oxide coatings, Wear 261 (11–12) (2006) 1298–1315.
[26] V. Cannillo, T. Manfredini, M. Montorsi, C. Siligardi, A. Sola, Microstructure-based modelling and experimental investigation of crack propagation in glass–alumina functionally graded materials, J. Eur. Ceram. Soc. 26 (15) (2006) 3067–3073.
[27] V. Cannillo, L. Lusvarghi, T. Manfredini, M. Montorsi, C. Siligardi, A. Sola, Analysis of crack propagation in alumina–glass functionally graded materials, in: Proceedings of the 16th European Conference of Fracture (ECF16), Alexandroupolis (Greece), July 3–7, 2006.
[28] Y. Kuromitsu, H. Yoshida, H. Takebe, K. Morinaga, Interaction between alumina and binary glasses, J. Am. Ceram. Soc. 80 (6) (1997) 1583–1587.
[29] G. Bolelli, V. Cannillo, L. Lusvarghi, T. Manfredini, C. Siligardi, C. Bartuli, A. Loreto, T. Valente, Plasma-sprayed glass–ceramic coatings on ceramic tiles: microstructure, chemical resistance and mechanical properties, J. Eur. Ceram. Soc. 25 (2005) 1835–1853.